Consequences of Breaking the Asp-His Hydrogen Bond of the Catalytic Triad: Effects on the Structure and Dynamics of the Serine Esterase Cutinase

Edmond Y. Lau and Thomas C. Bruice
Department of Chemistry, University of California, Santa Barbara, California 93106 USA

ABSTRACT The objective of this study has been to investigate the effects on the structure and dynamics that take place with the breaking of the Asp-His hydrogen bond in the catalytic triad Asp^{175}-His^{188}-Ser^{120} of the serine esterase cutinase in the ground state. Four molecular dynamics simulations were performed on this enzyme in solution. The starting structures in two simulations had the Asp^{175}-His^{188} hydrogen bond intact, and in two simulations the Asp^{175}-His^{188} hydrogen bond was broken. Conformations of the residues comprising the catalytic triad are well behaved during both simulations containing the intact Asp^{175}-His^{188} hydrogen bond. Short contacts of less than 2.6 Å were observed in 1.2% of the sampled distances between the carboxylate oxygens of Asp^{175} and the NE2 of His^{188}. The simulations showed that the active site residues exhibit a great deal of mobility when the Asp^{175}-His^{188} hydrogen bond is broken. In the two simulations in which the Asp^{175}-His^{188} hydrogen bond is not present, the final geometries for the residues in the catalytic triad are not in catalytically productive conformations. In both simulations, Asp^{175} and His^{188} are more than 6 Å apart in the final structure from dynamics, and the side chains of Ser^{120} and Asp^{175} are in closer proximity to the NE2 of His^{188} than to ND1. Nonlocal effects on the structure of cutinase were observed. A loop formed by residues 26–31, which is on the opposite end of the protein relative to the active site, was greatly affected. Further changes in the dynamics of cutinase were determined from quasiharmonic mode analysis. The frequency of the second lowest mode was greatly reduced when the Asp^{175}-His^{188} hydrogen bond was broken, and several higher modes showed lower frequencies. All four simulations showed that the oxyanion hole, composed of residues Ser^{42} and Gln^{121}, is stable. Only one of the hydrogen bonds (Ser^{42} OG to Gln^{121} NE2) observed in the crystal structure that stabilize the conformation of Ser^{42} OG persisted throughout the simulations. This hydrogen bond appears to be enough for the oxyanion hole to retain its structural integrity.

INTRODUCTION

The catalytic triad consisting of Ser-His-Asp/Glu is common to a class of hydrolytic enzymes. Serine proteases such as trypsin, elastase, α-lytic protease, and subtilisin have little structural homology and do not recognize the same substrate, yet each employs the catalytic triad to hydrolyze a peptide bond (Kraut, 1977; Steitz and Shulman, 1982). Overlaying of the catalytic residues shows that they occupy the same relative positions in each of the enzymes that contain this moiety. Serine proteases are highly efficient catalysts that accelerate reactions by a factor of up to 10^{10} over noncatalyzed reactions (Kraut, 1977).

The function of the serine is to enter into a transacylation reaction with the substrate to form an acyl-enzyme intermediate, which is then hydrolyzed to form the product. The role of the imidazole of histidine is to act as a general-base catalyst to remove the proton from the serine hydroxyl group in concert with the nucleophilic attack of the serine oxygen on the substrate acyl carbonyl carbon (Scheme 1). The importance of the carboxylic acid in the catalytic triad has been under debate for many years. In the charge relay hypothesis, which received almost universal acclaim, the ϵ nitrogen of the imidazole played the role of general base to assist serine attack on the substrate, and the role of the Asp-CO_2^- was to remove a proton (Scheme 1) from the δ-nitrogen of the imidazolium ion (Blow et al., 1969). The overall charge relay reaction (Scheme 2) is thermodynamically disfavored, however, because the aspartate is the much poorer base compared to the imdazole (Bruice, 1976). ^{15}N and ^{13}C NMR experiments on the catalytic histidine (Scheme 2) of α-lytic protease showed that the pKa of the residue is near 7.0, showing the charge relay to be unfavorable (Bachovchin, 1978, 1981). Calculations by Warshel and co-workers show that the transition state (TS) of the charge relay mechanism is 12 kcal/mol higher in energy relative to the TS containing both Asp and His charged (Warshel et al., 1989; Warshel, 1991). In addition, their calculations estimate a more than 4 kcal/mol increase in free energy in the TS when Asp is replaced by Ala. There have been proposals that the primary role of the Asp carboxylic group is to stabilize a required conformation of the histidine imidazole rather than to serve as a general-base catalyst. Rogers and Bruice were able to show in model compounds for the Ser-His-Asp triad of serine proteases that only a threefold rate enhancement could be attributed to the carboxylate group (Rogers and Bruice, 1974). This rate enhancement in solution is, of course, much less than observed experimentally for these enzymes. The authors speculated that the heterogeneity and the ordered surroundings of the triad functional groups at the active site may account for the

Received for publication 5 February 1999 and in final form 21 April 1999.
Address reprint requests to Dr. Thomas C. Bruice, Department of Chemistry, University of California, Santa Barbara, CA 93106. Tel.: 805-893-2044; Fax: 805-893-2229; E-mail: tcbruice@bioorganic.ucsb.edu.

0006-3495/99/07/85/14 $2.00

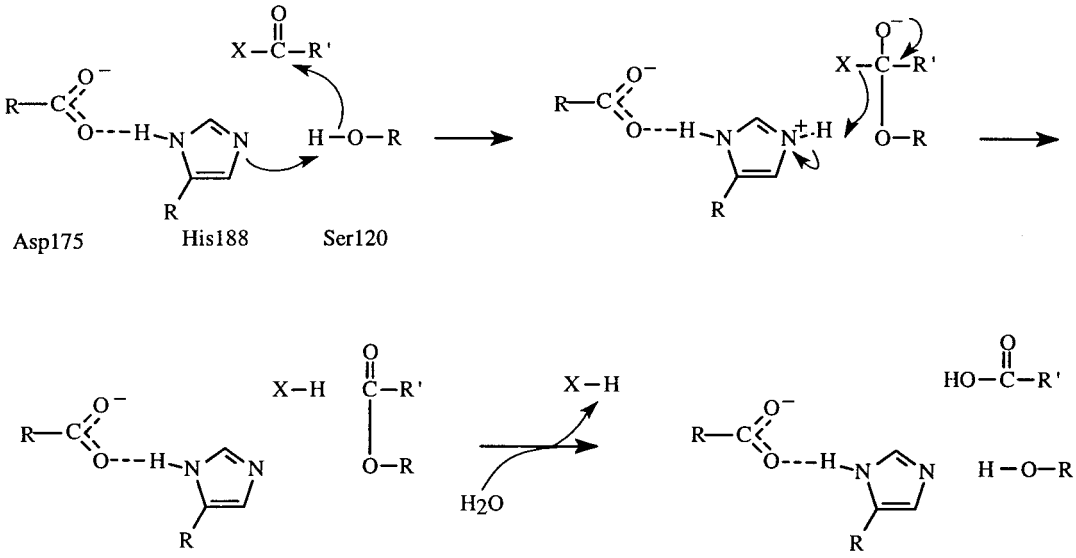

Scheme 1

rate enhancement. A similar conclusion was reached by Fersht and Sperling in their work with chymotrypsin and chymotrypsinogen (Fersht and Sperling, 1973). They observed that an intact catalytic triad exists within both chymotrypsin and chymotrypsinogen, yet only one is catalytically active. They postulated that the buried carboxylate may constrain the position of the imidazole and that the catalytic efficacy is due to a moderately reactive catalyst coupled with the substrate in a precise orientation. Obviously something special was missing in the charge relay concept.

Recently Frey, Cleland, and McCreevoy have suggested that the Asp-CO_2^- forms a low-barrier hydrogen bond (LBHB) with the histidine imidazole in serine proteases (Cleland and Kreevoy, 1994; Frey et al., 1994; Geralt et al., 1997). This proposal is based on an anomalous downfield shift of the ^{1}H NMR chemical shift observed for the amine hydrogen of the catalytic histidine. This far-downfield chemical shift has been observed in all serine proteases studied by proton NMR (Frey et al., 1994). This proton also has an extremely low fractionation value, which indicates that it is in a highly stable hydrogen bonding arrangement and is protected from solvent exchange. Arguments were presented that supported up to 20 kcal/mol resonance stabilization energy on the formation of a LBHB. Such a stabilization energy would provide a role for the aspartic acid member of the Asp-His-Ser triad in catalysis. This catalytic role for a LBHB is not universally accepted (Ash et al., 1997; Guthrie, 1996; Warshel et al., 1995). Warshel et al. have reject the role of LBHBs in proteins. Calculations by Warshel and co-workers using empirical valence bond theory have shown that transition states containing LBHBs are less stable than an ionic hydrogen bond ($Asp^-\cdots His^+$) in solution (Warshel and Papazyan, 1996). It has recently been shown, however, by a combination of experimental low-temperature (20 K) neutron diffraction and x-ray crystallographic measurements combined with high-level quantum mechanical calculations, that the low-barrier hydrogen bond in crystalline benzoylacetone is characterized by 16 kcal/mol resonance stabilization (Schiott et al., 1998). It is not known whether this molecule will form a LBHB in solution. It appears that much more research into LBHB will be forthcoming.

Warshel and co-workers have pointed out that (Warshel and Florian, 1998; Warshel, 1998) the reorganization energy of orientating polar groups in the enzyme active site is small, relative to the reaction in solution, because the dipoles are already positioned to interact with the TS. This preorganization has been proposed to suffice in explaining the efficency of the serine esterase enzymes. Their calculations of the change in free energy when the oxyanion hole is destabilized by mutation are in good agreement with experiment (Warshel et al., 1988, 1989).

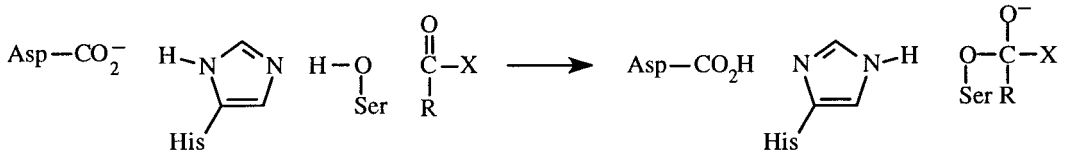

Scheme 2

The alkane dehalogenase of *Xanobactor autotrophicus* is responsible for the hydrolysis of 1,2-dichloroethane to 2-chloroethanol. This enzyme has at its active site a catalytic triad consisting of Asp^{124}, His^{289}, and H_2O. It has been shown recently, using computer simulations of the E·S complex, that the choice of the imidazole nitrogen (ND1 versus NE2) that is to be covalently bonded to a hydrogen can have significant consequences for the active site structure (Lightstone et al., 1998). When the proton resides on ND1, the active site residues are well behaved for the duration of the simulation, and conformations are found that would lead to catalysis. There are dramatic changes in the active site when the proton is moved to the NE2 position of the histidine imidazole. Productive conformations that can lead to catalysis cannot be formed. The stabilizing interaction formed between Asp^{124} and His^{289} when ND1 is protonated is disrupted when the hydrogen is moved to the NE2 position. The Asp^{124} is so affected by the breaking of the Asp^{124}-His^{289} hydrogen bond that it rotates out of the active site. The Asp^{124} side chain undergoes two consecutive rotations, which move it 9 Å away from the enzyme-bound substrate.

A study has now been initiated to determine the consequences of breaking the Asp-His hydrogen bond of a catalytic triad in a serine esterase enzyme. Cutinase from *Fusarium solani pisi,* with the catalytic triad Asp^{175}-His^{188}-Ser^{120} (Fig. 1), was chosen for this study. Cutinase hydrolyzes the ester linkages of triglycerides and cutin. Cutinase is a particularly good choice for our study because it is a relatively small, monomeric enzyme consisting of 214 residues, but the first 15 amino acids are not present in the mature enzyme. Many high-resolution crystal structures for this enzyme have been reported,and cutinase has recently been solved at 1.0 Å resolution (Longhi et al., 1997). The protein is a compact single-domain molecule with dimensions of $\sim 45 \times \sim 30 \times \sim 30$ $Å^3$. It contains a central β-sheet consisting of five parallel strands covered by five α-helices, the α/β hydrolase fold (Schrag and Cygler, 1997). Cutinase differs from true lipases in that it lacks a flap region that buries the hydrophobic binding site (Cygler and Schrag, 1997). This flap may prevent lipases from aggregating in solution. Cutinase also lacks interfacial activation as described for true lipases. Analogous to the serine proteases, cutinase contains an oxyanion hole consisting of the main-

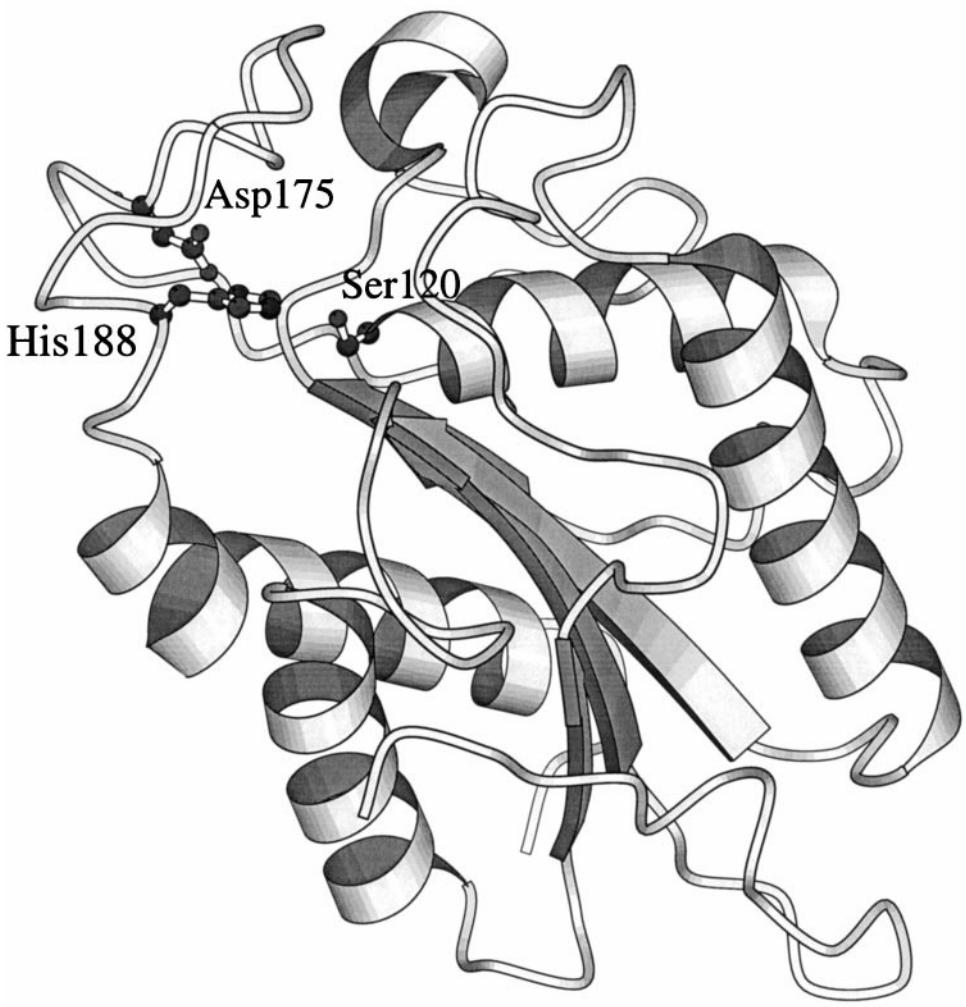

FIGURE 1 Schematic diagram of cutinase. The catalytic triad for this enzyme is represented in ball-and-stick format. This picture was made with the program MOLSCRIPT (Kraulis, 1991).

chain nitrogens of Ser^{42} and Gln^{121} and the OG atom of Ser^{42} (Martinez et al., 1994; Nicolas et al., 1996). Interestingly, unlike the other lipases, the oxyanion hole of cutinase is preformed (Martinez et al., 1994). In the other lipases, either structural rearrangement must occur or substrate must be bound for the oxyanion hole to form.

METHOD

Four molecular dynamics simulations were performed in this study. The crystal structure of cutinase solved at 1.25-Å resolution (Brookhaven Protein Data Bank entry 1CUS) and containing 197 amino acids (the first 16 residues were not included in the crystal structure) was used as the starting structure. Two simulations were performed on cutinase in which the imidazole proton was on ND1 of His^{188}. The only difference between these two simulations is in the initial seed value for the random number generator used for assignment of the initial velocities. In the other two simulations, the hydrogen bond between Asp^{175} and His^{188} of the catalytic triad was disrupted. In one of these simulations, the imidazole proton was on ND1 of His^{188} and the imidazole ring was rotated 180°, about the dihedral angle formed by CA-CB-CG-CD2, from its initial position in the crystal structure (denoted ROT). In the other simulation, the position of the imidazole ring of His^{188} in the crystal structure was utilized in the starting structure, but the hydrogen was placed on NE2 instead of ND1 (denoted HE2). Scheme 3 shows the relative geometries for the catalytic residues for the ROT and HE2 simulations. All four of these simulations correspond to the ground state for cutinase. The preparation for each cutinase model for a molecular dynamics simulation was the same and is detailed in Scheme 3.

The program CHARMM (versions 22.5 and 25b2) was used for all molecular dynamics simulations (Brooks et al., 1983). Hydrogen atoms were added to the crystal structure, including the crystallographic waters, by using CHARMM. The protein and crystallographic waters were solvated in a 35-Å-radius sphere (Chandrasekhar et al., 1992; Philippopoulos and Lim, 1995) of flexible TIP3P water (Jorgensen et al., 1983). Any water molecule within 2.8 Å of the protein or a crystallographic water was deleted. The total number of water molecules in each simulation varied slightly, but the system consisted of ~17,378 atoms (2867 protein atoms and 4837 water molecules). The potential energy of these systems (protein and water) was minimized by using a combination of steepest descents and adopted basis Newton-Raphson methods (Brooks et al., 1987). Molecular dynamics was performed on the energy-minimized system, and all systems were treated as microcanonical ensembles (NVE). The system was heated to 300 K in 5 ps and equilibrated for 30 ps. Production dynamics were performed for 500 ps. All analysis of the trajectories was done on the last 500 ps of dynamics. The Coulombic interactions were cut off at 12 Å by the use of a shifting function, and the van der Waals interactions were cut off by the use of a switching function between 10 and 11 Å (Brooks et al., 1983). The equations of motion were integrated using the Verlet algorithm with a time step of 1 fs (Verlet, 1967). The nonbonded list was updated every 10 time steps. All residues were modeled using the CHARMM all-atom parameter set (version 22) (MacKerell et al., 1998).

Positional fluctuations of the backbone atoms were calculated from the trajectories and compared to those obtained from the crystal structure. The fluctuations of the backbone atoms in the crystal structure were obtained by assuming that the Debye-Waller B-factors were free of contributions from lattice defects and the motions of the atoms were isotropic. The positional fluctuations of an atom can be obtained from the associated B-factors by using the equation $\langle \Delta r^2 \rangle^{1/2} = (3B/8\pi^2)^{1/2}$ (McCammon and Harvey, 1987).

The solvent-accessible surface area (SASA) of the protein was calculated with the program NACCESS (Hubbard and Thornton, 1993). Only the heavy atoms of cutinase were used for the calculations. Standard van der Waals radii were used for the heavy atoms in cutinase. A probe radius of 1.4 Å was used, and the slice thickness was 0.05 Å.

To study changes in the internal motions of cutinase due to breakage of the Asp^{175}-His^{188} hydrogen bond, quasiharmonic mode analysis was performed on the α carbons (CAs) in the protein to reduce the size of the displacement matrix (Teeter and Case, 1990; Verma et al., 1997). New trajectories for cutinase were generated from each original simulation. The CA of the cutinase in each of the original coordinate sets was overlayed with the energy-minimized structure by a least-squares fit to remove the rotational and transitional motions of the cutinase, and the new coordinates for cutinase were saved. The quasiharmonic modes of the CA were calculated using these new trajectories. The displacements from the principal axis were calculated directly from the new trajectories.

RESULTS AND DISCUSSION

To avoid confusion when describing the individual molecular dynamics simulations of cutinase, the trajectories will be referred to as follows: NAT is the simulation of cutinase with the imidazole proton on ND1 His^{188}. NAT2 is the replicate of simulation NAT, using the same starting minimized structure of cutinase but a different seed value for the random number generator used to assign the initial velocities. As seen in Scheme 3, HE2 refers to the simulation in which the NE2 of His^{188} is protonated, and ROT is the simulation in which the imidazole ring of His^{188} has been rotated and ND1 is protonated. All four simulations were stable over the duration of their trajectories. The ratio of the fluctuation of the total energy to the fluctuation of the kinetic energy was below 1% for each simulation, and the variation in the temperature was less than 5 K; thus differences observed in the dynamics are not due to instabilities in the simulations (Allen and Tildesley, 1987).

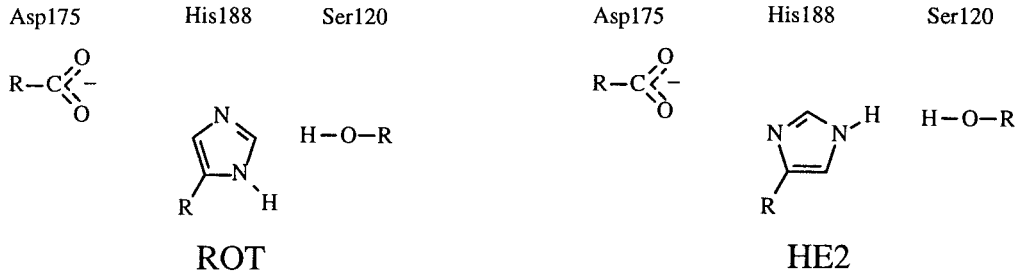

Scheme 3

Root mean squared deviations

The root mean squared deviations (RMSDs) of the backbone atoms (N, CA, and C) of cutinase during dynamics from the crystal structure were calculated for each trajectory. The RMSD of the cutinase in which the Asp^{175}-His^{188} hydrogen bond was broken resulted in a higher RMSD for the protein than in simulations of cutinase with an intact catalytic triad. This difference in RMSD between cutinase simulations was not a result of the energy minimization distorting one structure more than another, because there are only small differences between starting structures. The average RMSD for each CA in the protein between the minimized (starting) structure and the crystal structure was 0.59, 0.58, and 0.62 Å for NAT, HE2, and ROT, respectively. Even after the heating and equilibration phases, the RMSDs for all four simulations are of a similar value, but the RMSD increases steadily in the simulations in which the Asp^{175}-His^{188} hydrogen bond is broken during production dynamics (Fig. 2). In both simulations in which the Asp^{175}-His^{188} hydrogen bond is broken, the RMSD of the backbone atoms reached 2.3 Å from the crystal structure. In both simulations of cutinase with an intact catalytic triad, the RMSD plateaued at 1.8 Å relative to the crystal structure. It appears that the catalytic triad of cutinase not only is necessary for catalysis, but also has a stabilizing influence on this protein's structure.

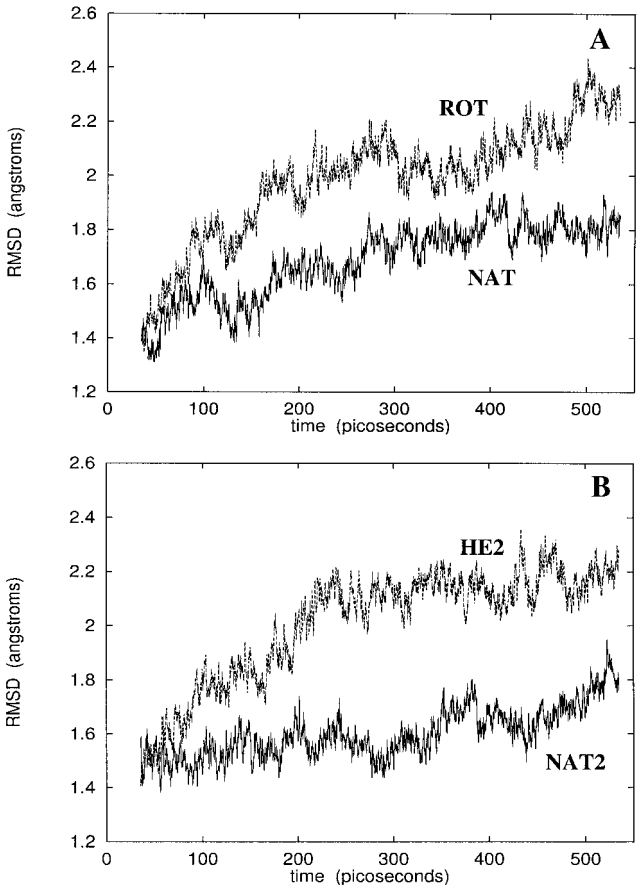

FIGURE 2 Root mean square deviations (RMSDs) of the backbone atoms (C, CA, and N) from the crystal structure during the simulation. (*A*) The RMSD for the ROT and NAT simulations. (*B*) The RMSD for HE2 and NAT2 simulations.

The greater RMSD in cutinase when the Asp^{175}-His^{188} hydrogen bond is broken is caused by large changes in the positions of the protein backbone in two regions, the solvent-exposed loop 26–31 and residues 170–200 (Fig. 3). Interestingly, these two regions are on opposite ends of the protein, which are separated by almost 30 Å. The change in positions of residues 170–200 can be directly related to breaking of the Asp^{175}-His^{188} hydrogen bond, because both residues reside in this region. This hydrogen bond appears to help stabilize the conformation of loop 180–188; once it is broken, Asp^{175} and His^{188} separate, which results in greater conformation flexibility. Loop 180–188 moves ~1 Å away from loop 80–88. Why loop 26–31 changes position is not readily apparent, because it is distant from the active site, but changes in this loop did occur in both simulations with the disrupted Asp^{175}-His^{188} hydrogen bond. It can be seen in Fig. 3 that loop 26–31 is a highly mobile region in cutinase, but when the Asp^{175}-His^{188} hydrogen bond is present, the conformation of the region is retained (Fig. 3 *A*, NAT simulation). Similar results are seen from the superimposition of the CA atoms of cutinase from the heteromorphous crystal structures (Longhi et al., 1996). There is a change in the conformation for residues 26–31 when the Asp^{175}-His^{188} hydrogen bond is broken (Fig. 3 *B*, ROT simulation). Similar results are obtained in the NAT2 and HE2 simulations. The initial change in position of the backbone atoms for ROT and HE2 in loop 26–31 from the energy minimization are no larger than changes observed for the native structures. The largest change in position for a CA in the NAT simulation in this region was 2.16 Å, and the majority of the displacements in the enzyme are well below this value (Fig. 4 *A*). The values from the NAT2 simulation for this region were less than the NAT simulation (Fig. 4 *B*). Some of the CAs in loop 26–31 move over 4 Å from their positions in the crystal structure when the Asp^{175}-His^{188} hydrogen bond is broken (Fig. 4, *C* and *D*). Although not well understood, it has been shown that loops distant from the active site can affect the rate of reaction in an enzyme. Mutational studies on Gly^{121} (located in a surface loop ~20 Å from the active site) of dihydrofolate reductase from *E. coli* have shown that this single change in a loop can affect both the conformation and rate of hydride transfer in the enzyme (Ohmae et al., 1996). The substrate specificity of chymotrypsin can be conferred on trypsin by mutation of trypsin's binding pocket. But the enzyme is not active unless two highly conserved surface loops in chymotrypsin replace two conserved loops in trypsin. The necessity of these two loops for activity is not readily apparent, because neither makes any contacts with the substrate (Hedstrom et al., 1992). It is intriguing that this distant loop in cutinase is affect by a perturbation in the active site.

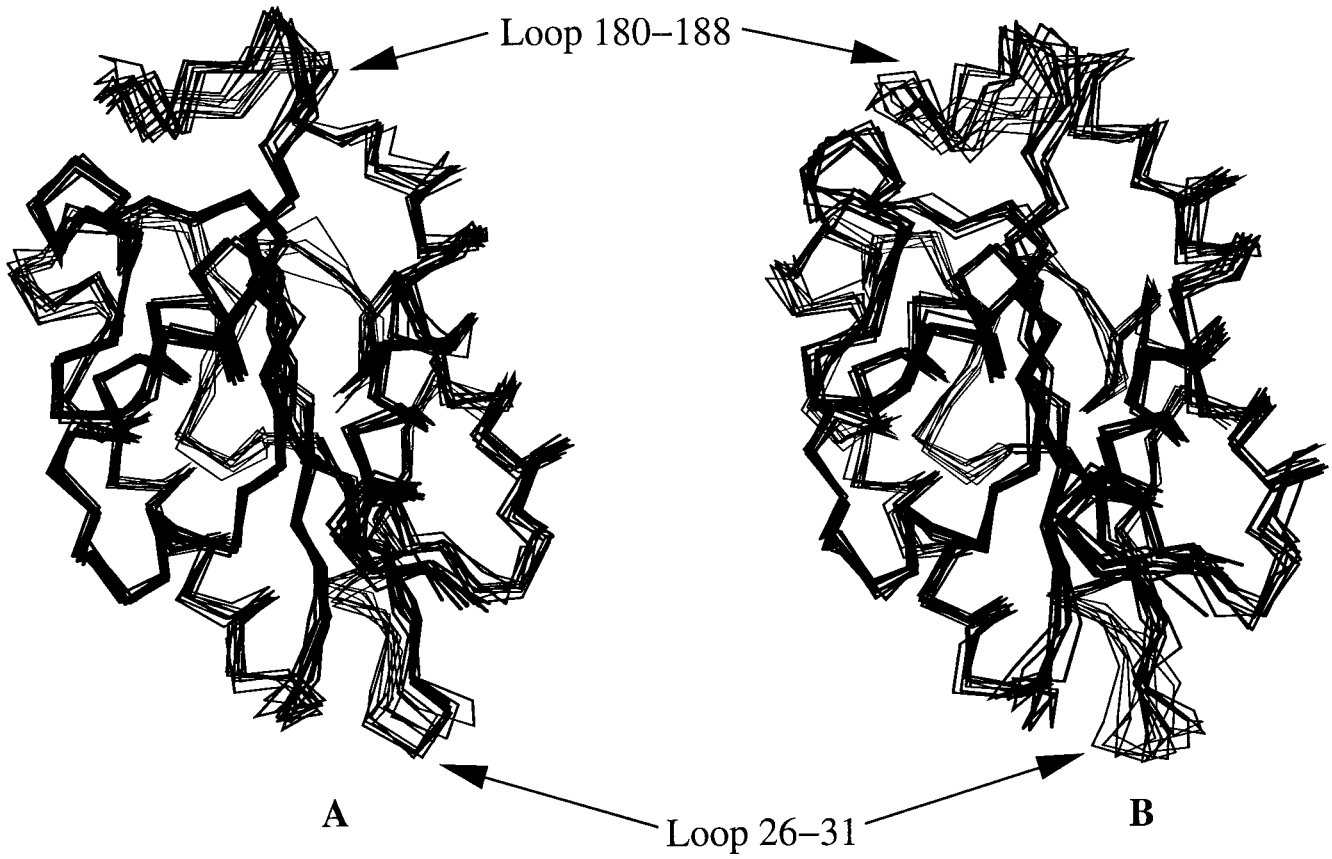

FIGURE 3 Superimposition of the α carbons of cutinase every 50 ps of the simulation for the NAT (*A*) and ROT (*B*) simulations.

The catalytic triad

The hydrogen bonds formed between the residues in the catalytic triad were stable throughout the simulations in which the Asp^{175}-His^{188} hydrogen bond was not broken. The Ser^{120} OG-to-His^{188} NE2 distances were 2.92 ± 0.17 and 2.92 ± 0.20 Å for the NAT and NAT2, respectively. The average distances between the carboxylate oxygens of Asp^{175} and ND1 of His^{188} were 3.00 ± 0.27 and 3.03 ± 0.23 Å for the NAT simulation. In the NAT2 simulation, the average distances were 2.87 ± 0.16 and 3.01 ± 0.18 Å for the carboxylate oxygen-to-ND1 distance. This indicates that in the NAT simulation, the carboxylate oxygens are in a bifurcated arrangement with ND1, but in NAT2 one oxygen is interacting with ND1 a majority of the time. Extremely short distances of less than 2.6 Å between the oxygens of Asp^{175}-CO_2^- and the imidazole nitrogen of His^{188} were found in the simulation. The total number of short contacts between an oxygen of Asp^{175} and the ND1 of His^{188} ($\leq$2.6 Å) is 1.2% of the sampled population for both of these ground-state simulations. Because measurable formation (^{1}H NMR) of LBHB in the serine proteases requires the presence of substrate (Frey et al., 1994; Geralt et al., 1997), it would have been interesting to compare distances obtained from a cutinase E · S complex to see if conformational changes occur in the enzyme that result in a greater percentage of the sampled population having a Asp^{175}-His^{188} hydrogen bond distance characteristic of LBHB. Unfortunately, there is no crystal structure of cutinase complexed with a model substrate. The importance of the observed population of short contacts between Asp^{175} and His^{188} is difficult to assess because cutinase only contains one histidine. Thus, direct comparisons with another Asp-His hydrogen bond in this enzyme are not possible. It should be noted that a LBHB or an ionic hydrogen bond (Warshel), which provides TS stabilization, will only form when an imidazolium ion and substrate are present.

In simulations that include the disrupted Asp^{175}-His^{188} hydrogen bond, there is a separation between these entities. The changes in the active site are not as drastic as seen in the alkane dehalogenase, where the aspartic acid rotated out of the active site when the histidine was protonated at the NE2 position (Lightstone et al., 1998). The aspartic acid did not rotate out of the active site in either cutinase simulation (ROT and HE2) that had a broken Asp^{175}-His^{188} hydrogen bond. The aspartic acid is unable to rotate out of the active site of cutinase because of a stabilizing interaction between it and Tyr^{191}. A hydrogen bond is formed between one of the carboxylate oxygens of Asp^{175} and the hydroxyl hydrogen of Tyr^{191}. This highly stable hydrogen bond is present in all four simulations and remains intact for the duration of

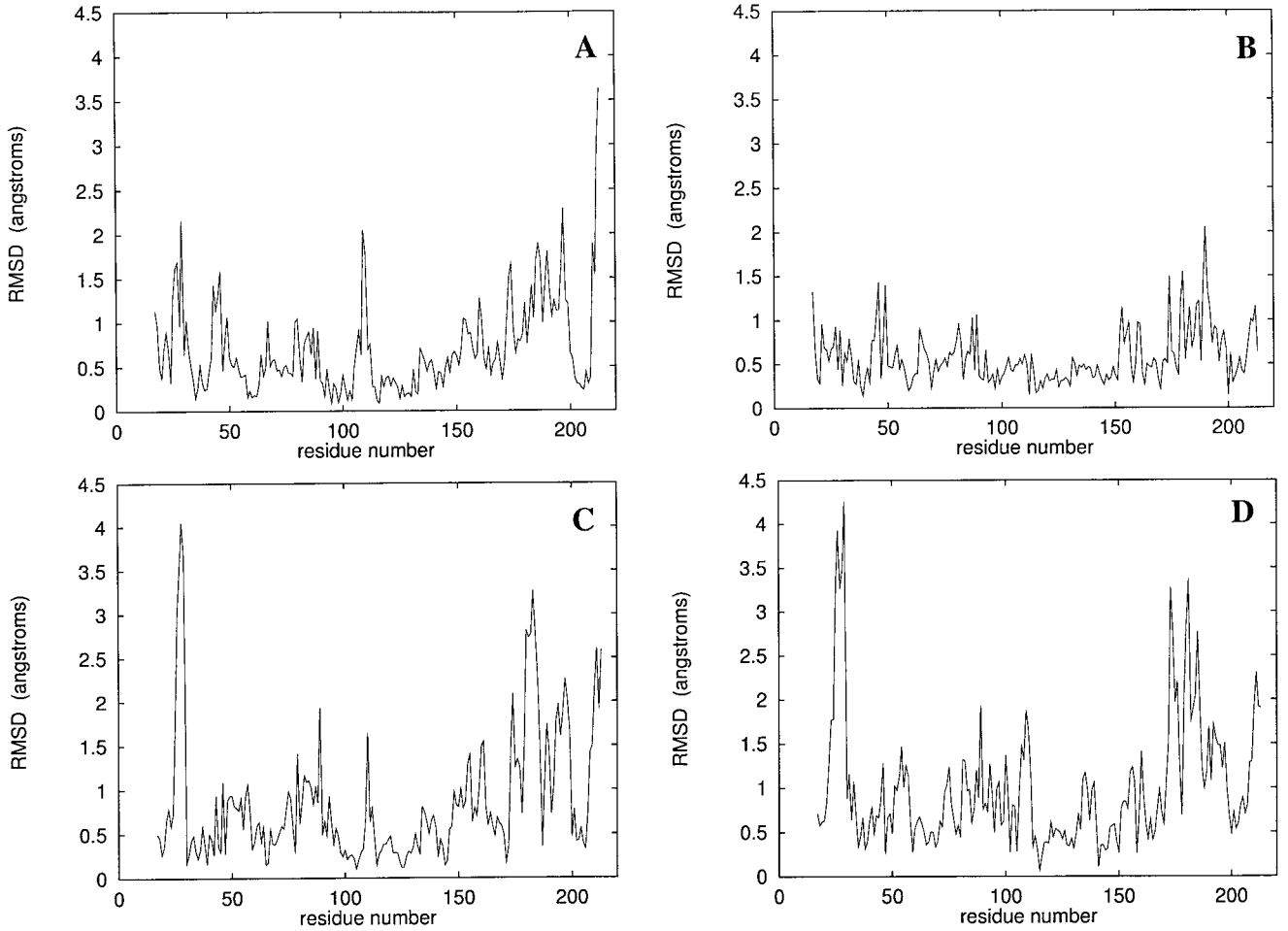

FIGURE 4 Root mean squared deviation between the α carbons of the average structure of cutinase from each simulation relative to the crystal structure.

the trajectory in all of the simulations performed. Interestingly, a similar interaction is formed in a simulation of trypsin. The catalytic Asp^{102} forms a hydrogen bond with the hydroxyl hydrogen of Tyr^{94} (study in progress).

There are drastic changes in the conformation of the catalytic residues when the hydrogen bond between Asp^{175} and His^{188} is broken. Not surprisingly, the separation between Asp^{175} and His^{188} increases greatly during the trajectories. The distances from the carboxylate oxygens to the nearest nitrogen in the imidazole in the ROT simulation increases from their initial separation of ~4 Å to a maximum distance of more than 8 Å (Fig. 5). In the case of the HE2 simulation, not only does the separation increase, but the histidine undergoes a ring flip of almost 180° (Fig. 6). Interestingly, rotation of the imidazole of the catalytic triad has also been observed in a double mutant of rat anionic trypsin (Asp^{102}-His^{57}-Ser^{195}). The crystal structure of trypsin D102S/S214D reveals that the imidazole ring is rotated by ~180° (about the CA-CB-CG-CD2 dihedral angle) from its position in the native enzyme (Corey et al., 1992). This alternative conformation for the trypsin mutant appears to be stabilized by interaction between OD2 of Asp^{214} and NE2 of His^{57}. Removal of the stabilizing influence of the Asp^{102}-His^{57} hydrogen bond allows the imidazole to rotate. In the HE2 trajectory of cutinase, a hydrogen bond, formed between the hydrogen attached to NE2 of His^{188} and OG of Ser^{120}, remains intact throughout the simulation. This hydrogen bond remains intact even with the altered conformation of the histidine, because of the relatively small change in position needed for the OG of Ser^{120} to remain in close contact with the hydrogen attached to NE2 in imidazole when the ring flip occurs. The hydroxyl oxygen of Ser^{120} only needs to undergo a dihedral transition (N-CA-CB-OG) to remain in close proximity to the HE2 of His^{188}.

In both simulations in which the Asp^{175}-His^{188} hydrogen bond is broken, the hydrogen attached to the nitrogen of the imidazole forms a very stable interaction with a solvent molecule. In the case of the HE2 simulation, the ND1 of the imidazole begins to interact strongly with a specific solvent molecule after the ring flip, which occurs at 135 ps (Fig. 7 *A*). This interaction is stable for the rest of the trajectory (400 ps). There is a similar occurrence in the ROT simulation. A distant water initially in the trajectory forms a very stable interaction with the ND1 of the imidazole during the last 100 ps of the simulation (Fig. 7 *B*). The conformation of the imidazole ring appears to be stable only when there is a

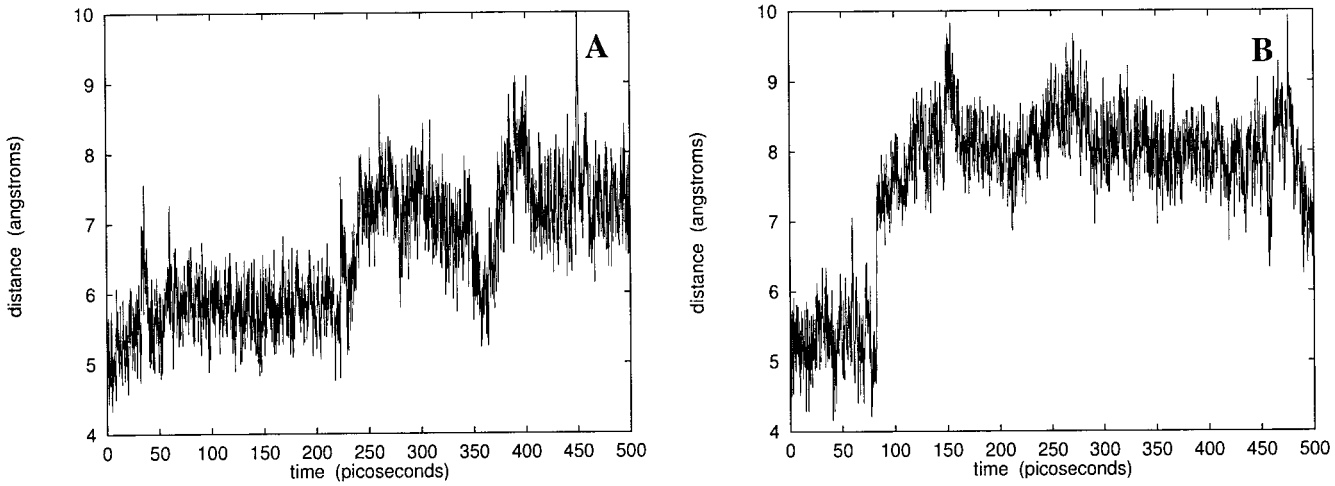

FIGURE 5 Separation between the Asp^{175} OD1 and the nearest nitrogen in the imidazole of His^{188} during the ROT (*A*) and HE2 (*B*) simulations.

strong interaction between a nitrogen and a highly polar group, either the carboxylate of Asp^{175} or a water molecule. In both the ROT and HE2 simulations, the final orientation of the imidazole ring is in a noncatalytic geometry (Fig. 8).

Positional fluctuations of the α carbons

The fluctuations of the CAs about their average positions during the trajectories can be compared directly to the Debye-Waller B-factors determined from x-ray crystallography. The average fluctuation for a CA is 0.65 Å, which is estimated from the crystal structure of cutinase solved recently at 1.0-Å resolution (Longhi et al., 1997). The calculated average fluctuations for the CA from these simulations are in good agreement with crystallography (Fig. 9). In the simulations with the native enzyme (intact catalytic triad), the calculated fluctuations for the CAs were 0.62 and 0.61 Å for NAT and NAT2, respectively. These values are also in agreement with a nanosecond simulation of cutinase using a different force field (GROMOS) and water model (SPC), which showed an average fluctuation of the α carbons of 0.60 Å from the dynamics and 0.72 Å when essential dynamics analyses were performed on the trajectory (Creveld et al., 1998; Longhi et al., 1996). In both simulations in which the Asp^{175}-His^{188} hydrogen bond is broken, there are larger fluctuations than seen with simulations of the native enzyme. The fluctuations for the HE2 and ROT simulations were both 0.66 Å. Although the average values for the fluctuations of the CA in the HE2 and ROT simulations are in better agreement with the results from crystallography than are the NAT and NAT2 simulations, it should be noted that fluctuations calculated from simulations tend to be less than those obtained by crystallography (Philippopoulos and Lim, 1995).

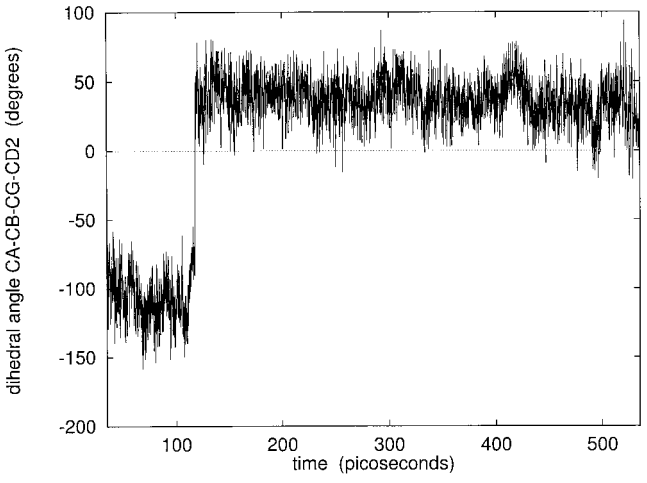

FIGURE 6 Plot of the dihedral angle for CA-CB-CG-CD2 of His^{188} in the HE2 simulation.

The fluctuations of the CAs in regions of secondary structure are similar for all of the simulations. Cutinase has a compact structure that consists of a five-stranded parallel β-sheet flanked by α-helices. The differences in the magnitudes of the fluctuations in the CAs arise from enhanced motions in the coils when the Asp^{175}-His^{188} hydrogen bond is broken. Three loops, comprising residues 26–31, 80–88, and 180–188, account for the majority of the differences in fluctuations between simulations. It can clearly be seen that the solvent-exposed loop 26–31 undergoes larger amplitude fluctuations when the catalytic hydrogen bond is broken than when it is intact (Fig. 9). The β-turn consisting of residues 109–112 also shows enhanced mobility when the Asp^{175}-His^{188} hydrogen bond is broken. The mobility in this turn is caused by contact with loop 26–31.

Interestingly, the residues in loop 80–88, which forms half of the lid of the active site, shows greater mobility when the catalytic hydrogen bond is intact. Loop 180–188, which forms the other half of the lid for the active site, shows a great deal of mobility in three of the four simulations; only the NAT2 simulation showed reduced fluctuations. The fluctuations for this loop in the NAT simulation are greater than those found from the crystal structure (Fig. 9 *A*). In the

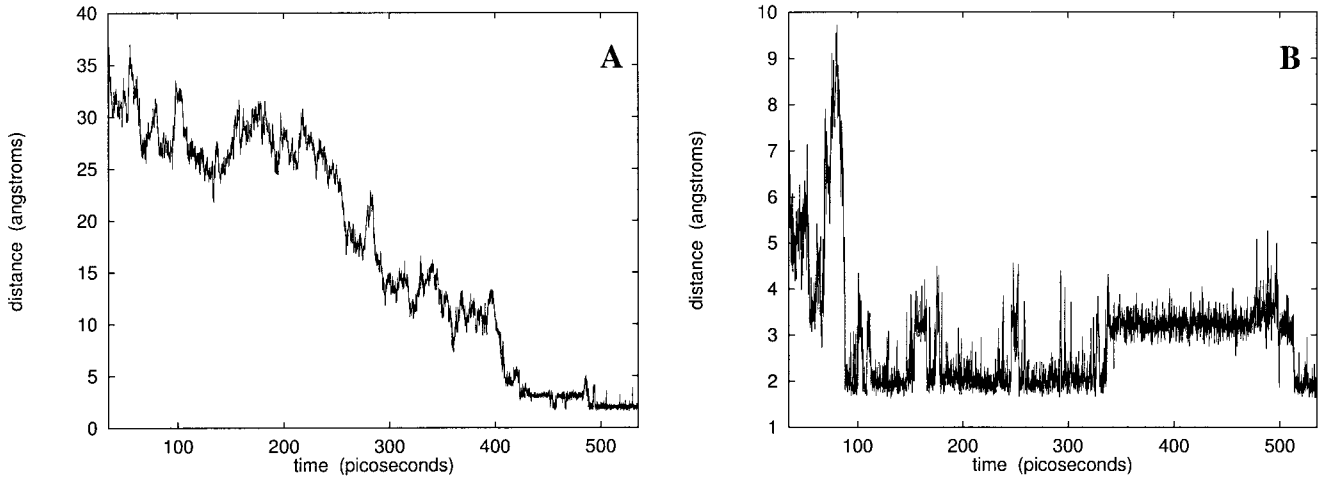

FIGURE 7 Distances between a stabilizing water molecule and ND1 of His^{188} in the ROT (*A*) and HE2 (*B*) simulations.

NAT simulation the fluctuations in loop 180–188 are of the same magnitude as those found in the simulations in which the Asp^{175}-His^{188} hydrogen bond is broken. All hydrogen bonds in the catalytic triad remain intact throughout the NAT simulation, which suggests that the active site of cutinase is flexible.

The oxyanion hole

Cutinase has an oxyanion hole to stabilize the developing negative charge on the substrate ester or amide carbonyl oxygen during the formation of the tetrahedral intermediate to acyl transfer. The oxyanion hole is vital for catalysis in serine proteases. Mutational and computational studies on subtilisin show a ~5.0 kcal/mol increase in free energy when Asn^{155}, which stabilizes the oxyanion hole conformation, is replaced by Ala (Warshel et al., 1988; Wells et al., 1986). A similar value is obtained from calculation for destabilizing the oxyanion hole of rat trypsin by a Gly-to-Ala double mutation (Warshel et al., 1988). Comparison of the crystal structures of cutinase without substrate and covalently inhibited by diethyl-*p*-nitrophenyl phosphate showed that there is little change in the overall structure of cutinase (Martinez et al., 1994). The residues forming the oxyanion hole in cutinase (Gln^{121} and Ser^{42}) occupy the same positions in the two crystal structures, which implies that unlike other lipases, cutinase has a preformed oxyanion hole. In addition to using the backbone amides of Gln^{121} and Ser^{42}, cutinase also utilizes the OG of Ser^{42} to form its oxyanion hole (Fig. 10 *A*). This differs from typical serine

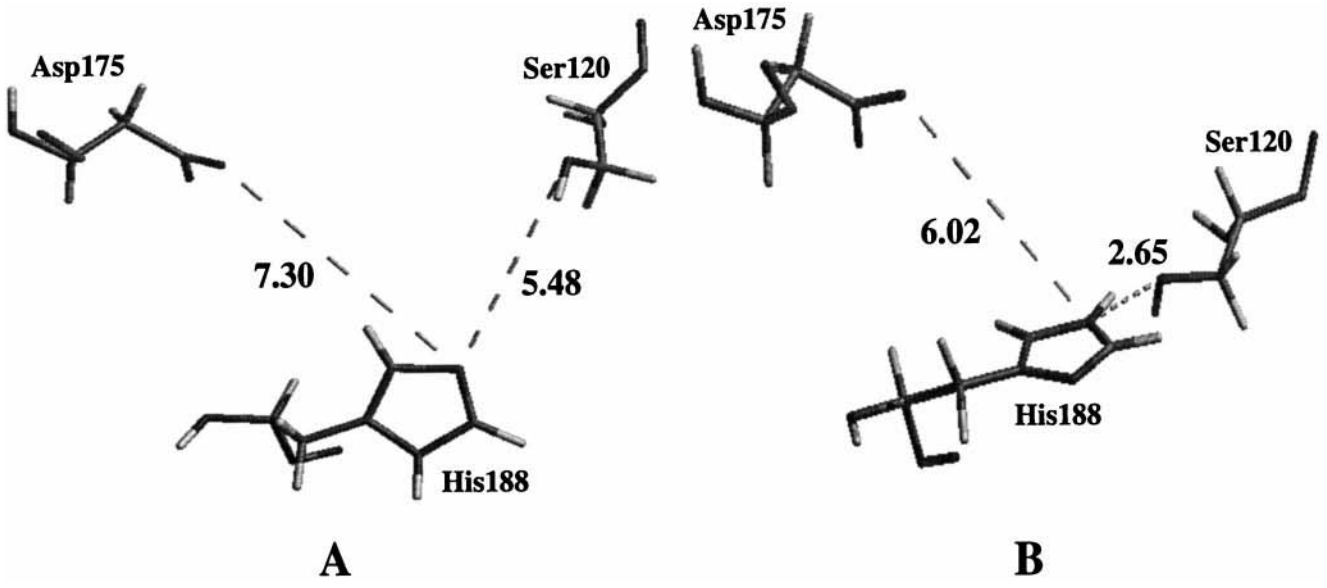

FIGURE 8 Final geometries for the residues in the catalytic triad from the ROT (*A*) and HE2 (*B*) simulations. The dashes show the shortest distances between a carboxylate oxygen and a nitrogen in the imidazole and between OG of Ser^{120} and a nitrogen in the imidazole. In both simulations, NE2 of His^{188} was the closest nitrogen to the side-chain oxygens of Asp^{175} and Ser^{120}. Values are in Ångstroms.

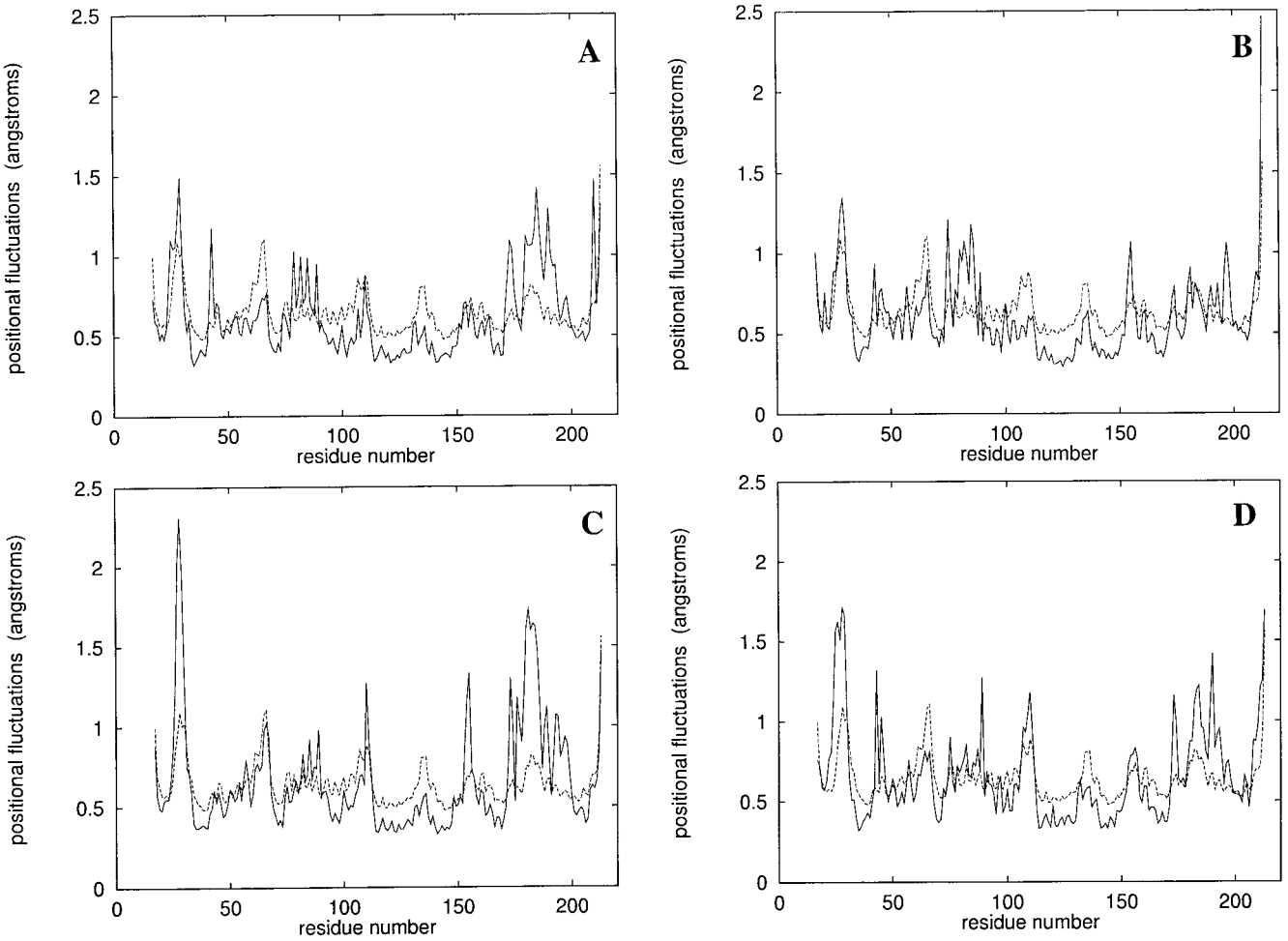

FIGURE 9 Positional fluctuations of the α carbons from the simulations (——) and from the 1.0-Å crystal structure (– – –). The NAT, NAT2, ROT, and HE2 simulations are shown in *A*, *B*, *C*, and *D*, respectively.

proteases, which use only the two backbone amides to form the oxyanion hole. The orientation of OG in Ser^{42} is stabilized in the crystal structure by hydrogen bonds between it and Gln^{121} NE2 and Asn^{84} ND2 (Nicolas et al., 1996). The distances between the OG of Ser^{42} and Gln^{121} NE2 and Asn^{84} ND2 are 3.15 and 3.06 Å, respectively, in the crystal structure. The behaviors of these two hydrogen bonds in the oxyanion hole are similar in all four simulations. The hydrogen bond between the Ser^{42} OG and Gln^{121} NE2 is stable and remains intact in all four simulations. The average separation between the Ser^{42} OG and the closest amide hydrogen of Gln^{121} ranged from a low of 2.25 Å in the ROT simulation to a high of 2.70 Å for the HE2 simulation (Fig. 11 *A*). The other hydrogen bond between Ser^{42} OG and Asn^{84} ND2 is unstable in all simulations performed. At initiation of each of the four simulations, the separation between Ser^{42} OG and Asn^{84} ND2 is well below 3 Å, but the hydrogen bond is not stable and breaks in the course of each simulation (Fig. 11 *B*). This hydrogen bond lasted for the longest amount of time (125 ps) in the ROT simulation; in the HE2 simulation the hydrogen bond breaks almost as soon as the simulation begins, and the separation increases to almost 10 Å during the trajectory. The stability of this hydrogen bond is consistent with results from x-ray crystallography. The side chain of Asn^{84} was found to be in a dual conformation in the 1.0-Å crystal structure. One conformation has a separation between Ser^{42} OG and Asn^{84} ND1 of 3.06 Å. The other conformation has the two atoms separated by 3.96 Å, and it does not appear that this conformation can provide stabilization for the orientation of the Ser^{42} OG atom. The B-factors from crystallography for atoms OG of Ser^{42}, NE2 of Gln^{121}, and ND2 of Asn^{84} are in agreement with the simulations. The values for OG of Ser^{42} and NE2 of Gln^{121} were 12.43 and 10.96 $Å^2$, respectively, for the 1.0-Å crystal structure (Longhi et al., 1997). The ND2 of Asn^{84} was found to be in dual positions in the same crystal structure, and the B-factors for each position (16.21 and 14.13 $Å^2$) were greater than for the atoms of Ser^{42} and Gln^{121}. Although the hydrogen bond between OG of Ser^{42} and ND2 of Asn^{84} is not stable, the relative conformation of OG is unaffected (Fig. 10 *B*). The single hydrogen bond between the side chains of Ser^{42} and Gln^{121} appears to be enough to preserve the oxyanion hole. Interestingly, the positional fluctuations in three of the four

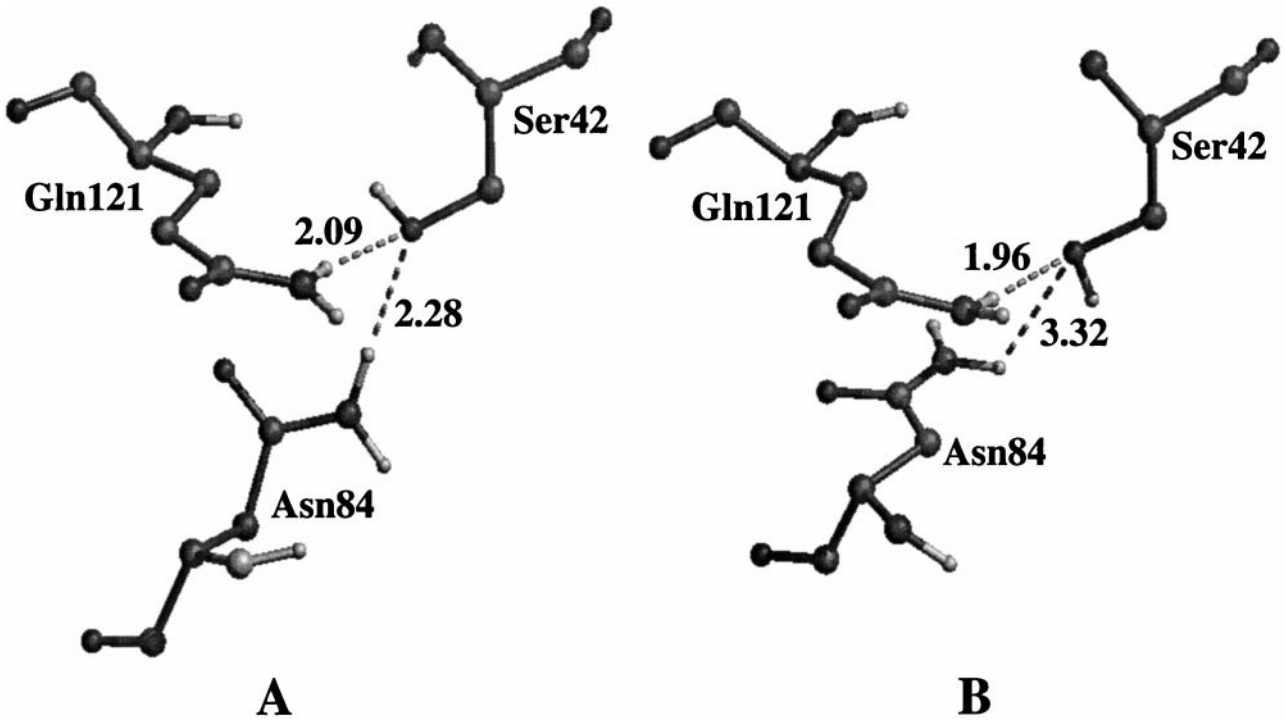

FIGURE 10 Diagram showing the relative positions of the residues forming the oxyanion hole in the crystal structure (*A*) and in the final structure from the NAT simulation (*B*). The distances are from the closest amide hydrogens of Gln^{121} and Asn^{84} to OG of Ser^{42}. All values are in Ångstroms. Only hydrogens attached to heavy polar atoms are shown.

simulations show greater motion in the backbone for residues 42–45 than the values estimated from the B-values. Only the ROT simulation had fluctuations of a value similar to those from crystallography. The calculated positional fluctuations for Gln^{121} are not significantly different from those from crystallography. NMR studies of cutinase indicate that the oxyanion hole is mobile from observed exchange broadening of the chemical shifts of Ser^{42} and Gln^{121} (Prompers et al., 1997). The large fluctuations in the protein backbone could be one of the causes for the exchange broadening. Even though the backbone of cutinase is mobile at residues 42–45, the oxyanion hole remains intact.

Solvent-accessible surface area

SASA is a sensitive method for monitoring changes in the structure of a protein. The α/β hydrolyase fold of cutinase

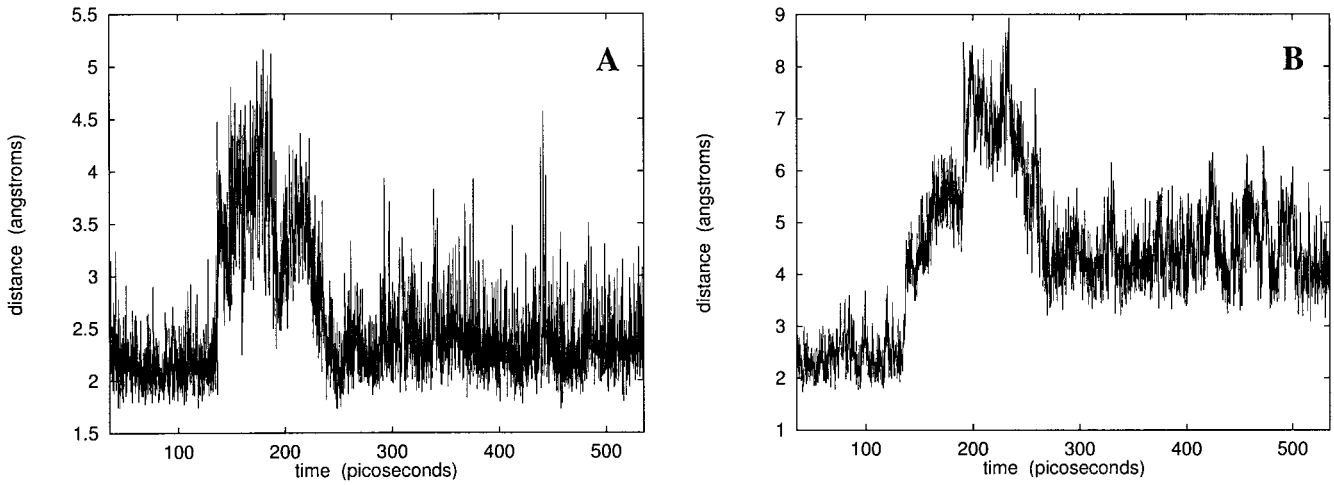

FIGURE 11 Distance between the closest amide hydrogen of Gln^{121} and OG of Ser^{42} of the oxyanion hole (*A*). (*B*) The separation between the closest amide hydrogen of Asn^{84} and OG of Ser^{42}. Both plots are from the NAT simulation.

TABLE 1 Average solvent-accessible surface area of cutinase*

	Total	Side chains	Main chain	Hydrophilic	Hydrophobic
NAT	8786	7511	1275	5023	3763
NAT2	8734	7499	1235	4908	3826
ROT	8989	7646	1343	5030	3959
HE2	8996	7641	1355	5061	3935
Xtal#	8460	7185	1275	4723	3736

*All values are in $Å^2$.
#Crystal structure of cutinase solved at 1.25 Å resolution (1CUS).

is a tight structural motif causing large-scale burial of residues, making them inaccessible to solvent (Table 1). There is only a modest increase of ~300 $Å^2$ in the total SASA in the two simulations with the intact catalytic triad relative to the value for the crystal structure (8460 $Å^2$). The average SASAs for cutinase calculated from the NAT and NAT2 simulations, 8734 $Å^2$ and 8786 $Å^2$, respectively, are in good agreement. When the Asp^{175}-His^{188} hydrogen bond is broken, the total SASA for cutinase increases by ~200 $Å^2$ (8996 and 8989 $Å^2$ for HE2 and ROT, respectively) relative to the native simulations. In both simulations with the nondisrupted catalytic triad, the total SASAs of the main-chain and hydrophobic atoms have almost exactly the same value as calculated from the crystal structure. This indicates that the increases in SASA for the native simulations are due to the side chains of hydrophilic residues becoming more solvent exposed, which is a favorable situation. When the Asp^{175}-His^{188} hydrogen bond is broken, the SASAs for the backbone atoms increase by ~100 $Å^2$ relative to the native simulations and the crystal structure. There is also a change in the average SASA for the hydrophobic atoms in cutinase: an increase of ~150 $Å^2$.

The majority of the change in SASA of cutinase when the Asp^{175}-His^{188} hydrogen bond is broken is located in three loops. Two loops comprising residues 80–88 and 180–188 are at the active site, and loop 26–31 is located at the opposite end of the protein. Although the values of the SASAs of the loops are not the same in each simulation, the sum of the SASAs for the three loops is in good agreement.

Quasiharmonic mode analysis

To further assess the motion that the backbone of cutinase is undergoing, quasiharmonic mode analysis was used to study the magnitude of the motions and their frequencies (Table 2). The 20 lowest mode frequencies calculated for the CAs from quasiharmonic analysis are in good agreement with similar simulations, and the values obtained for the NAT and NAT2 are in good agreement, as are the values of the ROT and HE2 simulations. The two simulations of cutinase containing the intact catalytic triad had very similar quasiharmonic modes; the difference in values between the 20 lowest frequency modes are on the order of 1 cm^{-1}. The variability in the calculated frequencies (~1 cm^{-1}) is the same for the two simulations in which the Asp^{175}-His^{188} hydrogen bond is broken. There are differences in the quasiharmonic modes of cutinase whether the Asp^{175}-His^{188} hydrogen bond is intact or broken. When broken, the second lowest mode in cutinase is significantly decreased. There is an almost 2.5 cm^{-1} decrease between the average value between the native simulations and the broken hydrogen bond simulations, indicating enhanced motions in the protein backbone. The largest displacements for this mode are centered in loop 26–31 and loop 180–188. There are also differences in values between a number of higher frequency modes, depending on whether the catalytic triad is intact. Modes 8–17 are 1–3 cm^{-1} less in cutinase with the broken Asp^{175}-His^{188} hydrogen bond relative to the native simulations. The displacements of the CA in cutinase from the lowest frequency mode in the simulations in which the Asp^{175}-His^{188} hydrogen bond was broken are much larger throughout the protein than when it is intact. Interestingly, the regions that showed the largest amplitude displacement in the HE2 and ROT simulations differed. In the HE2 simulation, the displacements of loop 26–31 dominate within cutinase; the amplitude of the fluctuations are greater than 1 Å for each CA within this loop. There are also significant fluctuations in loop 80–88 and in the turn formed by residues 108–111. In the ROT simulation, large-

TABLE 2 The 20 lowest frequency modes calculated from quasiharmonic mode analysis*

	NAT	NAT2	ROT	HE2
1	4.64	5.02	4.26	4.29
2	9.30	8.02	5.54	6.58
3	10.58	10.94	9.06	10.32
4	13.44	12.23	12.50	12.17
5	14.31	13.51	14.52	13.56
6	15.43	14.43	15.46	13.96
7	16.94	16.99	16.15	16.91
8	19.17	19.64	17.80	18.12
9	20.93	21.24	18.53	18.78
10	21.97	21.72	19.37	19.74
11	23.49	23.17	20.90	20.12
12	25.19	24.59	21.96	22.76
13	25.45	25.79	23.03	23.71
14	26.30	25.96	24.31	24.65
15	27.60	26.40	25.51	25.23
16	28.22	28.20	26.60	26.67
17	28.72	28.76	27.74	27.61
18	29.10	29.68	28.26	29.69
19	29.53	31.08	28.64	30.79
20	30.20	31.59	29.85	30.97

*All values are in cm^{-1}.

amplitude motions are observed in the two lowest frequency modes. In the lowest frequency mode, the motions in the loop 180–188 are more than twice those observed for most of the CAs in cutinase for this simulation. Interestingly, the motions of loop 26–31 in mode 2 are the largest observed in this simulation of cutinase.

CONCLUSIONS

These molecular dynamics simulations of cutinase have been able to show that not only does Asp^{175} orient the imidazole of His^{188} in the catalytic triad, but it has an important role in stabilizing the local structure around the active site. A similar conclusion was reached by Quirk et al. for ribonuclease A (RNase A) from mutational studies of the enzyme's His-Asp catalytic dyad (Quirk et al., 1998). Replacement of the catalytic Asp^{121} in RNase A with either Asn or Ala resulted in a 2.0 kcal/mol decrease, from a total of 9.0 kcal/mol, in conformational stability at pH 6.0. When the triad Asp^{175}-His^{188} hydrogen bond of cutinase was broken, three flexible loops in the protein were greatly affected, leading to large-scale fluctuations and a widening of the lid of the active site. The separation between Asp^{175} and His^{188} increased in both simulations, and the final geometry of the imidazole ring was in a noncatalytic conformation. Although ~30 Å away from the active site, the loop formed by residues 26–31 showed enhanced mobility and a change in conformation when the Asp^{175}-His^{188} hydrogen bond was broken.

The stability of the oxyanion hole of cutinase is not dependent upon the integrity of the Asp^{175}-His^{188} hydrogen bond. Only one of two hydrogen bonds (Ser^{42} OG to Gln^{121} NE2) observed in the crystal structure that stabilize the orientation of OG persisted throughout the simulations. This one hydrogen bond is enough for the oxyanion hole to retain its structural integrity.

The authors thank the referees for their helpful comments on the manuscript. The authors are grateful for computer time on UCSB's SGI Origin 2000, which is partially supported by grants from the National Science Foundation (CDA96-01954) and Silicon Graphics, and Prof. Martin Karplus for providing a copy of the program CHARMM (version 25b2).

This study was supported by grant MCB-9727937 from the National Science Foundation.

REFERENCES

Allen, M. P., and D. J. Tildesley. 1987. Computer Simulation of Liquids. Clarendon, Oxford.

Ash, E. L., J. L. Sudmeier, E. C. De Fabo, and W. W. Bachovchin. 1997. A low-barrier hydrogen bond in the catalytic triad of serine proteases? Theory versus experiment. *Science.* 278:1128–1132.

Bachovchin, W. W., R. Kaiser, J. H. Richards, and J. D. Roberts. 1981. Catalytic mechanism of serine protease: reexamination of the pH dependence of the histidyl $^1J^{13}_{C\text{-}H}$ coupling constant in the catalytic triad of α-lytic protease. *Proc. Natl. Acad. Sci. USA.* 78:7323–7326.

Bachovchin, W. W., and J. D. Roberts. 1978. Nitrogen-15 nuclear magnetic resonance spectroscopy. The state of histidine in the catalytic triad of α-lytic protease. Implications for the charge-relay mechanism of peptide-bond cleavage by serine proteases. *J. Am. Chem. Soc.* 100: 8041–8047.

Blow, D. M., J. J. Birktoft, and B. S. Hartlet. 1969. Role of a buried acid group in the mechanism of action of chymotrypsin. *Nature.* 221: 337–340.

Brooks, B. R., R. E. Bruccoleri, B. D. Olafson, D. J. States, S. Swaminathan, and M. Karplus. 1983. CHARMM: a program for macromolecular energy, minimization, and dynamics calculations. *J. Comput. Chem.* 4:187.

Brooks, C. L., III, M. Karplus, and B. M. Pettitt. 1987. Proteins: A Theoretical Perspective of Dynamics, Structure, and Thermodynamics. John Wiley and Sons, New York.

Bruice, T. C. 1976. Some pertinent aspects of mechanisms as determined with small molecules. *Annu. Rev. Biochem.* 45:331–373.

Chandrasekhar, I., G. M. Clore, A. Szabo, A. M. Gronenborn, and B. R. Brooks. 1992. A 500 ps molecular dynamics simulation study of interleukin-1β in water. *J. Mol. Biol.* 226:239–250.

Cleland, W. W., and M. M. Kreevoy. 1994. Low-barrier hydrogen bonds and enzymatic catalysis. *Science.* 264:1887–1890.

Corey, D. R., M. E. McGrath, J. R. Vasquez, R. J. Fletterick, and C. S. Craik. 1992. An alternative geometry for the catalytic triad of serine proteases. *J. Am. Chem. Soc.* 114:4507–4509.

Creveld, L. D., A. Amadei, R. C. van Schaik, H. A. M. Pepermans, J. de Vlieg, and H. J. C. Berendsen. 1998. Identification of functional and unfolding motions of cutinase as obtained from molecular dynamics computer simulations. *Proteins.* 33:253–264.

Cygler, M., and J. D. Schrag. 1997. Structure as basis for understanding interfacial properties of lipases. *Methods Enzymol.* 284:3–27.

Fersht, A. R., and J. Sperling. 1973. The charge relay system in chymotrypsin and chymotrypsinogen. *J. Mol. Biol.* 74:137–149.

Frey, P. A., S. A. Whitt, and J. B. Tobin. 1994. A low-barrier hydrogen bond in the catalytic triad of serine proteases. *Science.* 264:1927–1930.

Geralt, J. A., M. M. Kreevoy, W. W. Cleland, and P. A. Frey. 1997. Understanding enzymatic catalysis: the importance of short, strong, hydrogen bonds. *Chem. Biol.* 4:259–267.

Guthrie, J. P. 1996. Short strong hydrogen bonds: can they explain enzymatic catalysis? *Chem. Biol.* 3:163–170.

Hedstrom, L., L. Szilagyi, and W. J. Rutter. 1992. Converting trypsin to chymotrypsin: the role of surface loops. *Science.* 255:1249–1253.

Hubbard, S. J., and J. M. Thornton. 1993. NACCESS. Department of Biochemistry and Molecular Biology, University College, London.

Jorgensen, W. L., J. Chandrasekhar, J. D. Madura, R. W. Impley, and M. L. Klein. 1983. Comparison of simple potential functions for simulating water. *J. Chem. Phys.* 79:926–935.

Kraulis, P. J. 1991. MOLSCRIPT: a program to produce both detailed and schematic plots of protein stuctures. *J. Appl. Crystallogr.* 24:946–950.

Kraut, J. 1977. Serine proteases: structure and mechanism of catalysis. *Annu. Rev. Biochem.* 46:331–358.

Lightstone, F. C., Y-J. Zheng, and T. C. Bruice. 1998. Molecular dynamics simulations of ground and transition states for the S_N2 displacement of Cl^- from 1,2-dichloroethane at the active site of *Xanthobacter autotrophicus* haloalkane dehalogenase. *J. Am. Chem. Soc.* 120:5611–5621.

Longhi, C. M., V. Lamzin, A. Nichols, and C. Cambillau. 1997. Atomic resolution (1.0 Å) crystal structure of *Fusarium solani* cutinase: stereochemical analysis. *J. Mol. Biol.* 268:779–799.

Longhi, S., A. Nicolas, L. Creveld, M. Egmond, C. T. Verrips, J. de Vlieg, C. Martinez, and C. Cambillau. 1996. Dynamics of *Fusarium solani* cutinase investigated through structural comparisons among different crystal forms of its variants. *Proteins.* 26:442–458.

MacKerell, A. D., Jr., D. Bashford, M. Bellott, R. L. Dunbrack, Jr., J. D. Evanseck, M. J. Field, S. Fischer, J. Gao, H. Guo, S. Ha, D. Joseph-McCarthy, L. Kuchnir, K. Kuczera, F. T. K. Lau, C. Mattos, S. Michnick, T. Ngo, D. T. Nguyen, B. Prodhom, W. E. Reiher, III, B. Roux, M. Schlenkrich, J. C. Smith, R. Stote, J. Straub, M. Watanabe, J. Wiorkiewicz-Kuczera, D. Yin, and M. Karplus. 1998. All-atom empirical potential for molecular modeling and dynamics studies of proteins. *J. Phys. Chem. B.* 102:3586–3616.

Martinez, C., A. Nicholas, H. van Tilbeurgh, M. P. Egloff, C. Cudrey, R. Verger, and C. Cambillau. 1994. Cutinase, a lipolytic enzyme with a preformed oxyanion hole. *Biochemistry.* 33:83–89.

McCammon, J. A., and S. C. Harvey. 1987. Dynamics of Proteins and Nucleic Acids. Cambridge University Press, Cambridge.

Nicolas, A., M. Egmond, C. T. Verips, J. de Vlieg, S. Longhi, C. Cambillau, and C. Martinez. 1996. Contribution of cutinase serine 42 side-chain to the stabilization of the oxyanion transition state. *Biochemistry.* 35:398–410.

Ohmae, E., K. Iriyama, S. Ichihara, and K. Gekko. 1996. Effects of point mutants at the flexible loop glycine-67 of *Escherichia coli* dihydrofolate reductase on its stability and function. *J. Biochem.* 119:703–710.

Philippopoulos, M., and C. Lim. 1995. Molecular dynamics simulation of *E. coli* ribonuclease H1 in solution: correlation with NMR and x-ray data and insights into biological function. *J. Mol. Biol.* 254:771–792.

Prompers, J. J., A. Groenewegen, R. C. Van Schaik, H. A. M. Pepermans, and C. W. Hilbers. 1997. ^{1}H, ^{13}C, and ^{15}N resonance assignments of *Fusarium solani pisi* cutinase and preliminary features of the structure in solution. *Protein Sci.* 6:2375–2384.

Quirk, D. J., C. Park, J. E. Thompson, and R. T. Raines. 1998. His-Asp catalytic dyad of ribonuclease A: conformational stability of the wild-type, D121N, D121A, and H119A enzymes. *Biochemistry.* 37: 17958–17964.

Rogers, G. A., and T. C. Bruice. 1974. Synthesis and evaluation of a model for the so-called "charge-relay" system of the serine esterase. *J. Am. Chem. Soc.* 96:2473–2481.

Schiott, B., B. B. Iversen, G. K. Hellerup Madsen, and T. C. Bruice. 1998. Characterization of the short strong hydrogen bond in benzoylacetone by Ab initio calculations and accurate diffraction experiments. Implications for the electronic nature of low-barrier hydrogen bonds in enzymatic reactions. *J. Am. Chem. Soc.* 120:12117–12124.

Schrag, J. D., and M. Cygler. 1997. Lipases and α/β hydrolase fold. *Methods Enzymol.* 284:85–107.

Steitz, T. A., and R. G. Shulman. 1982. Crystallographic and NMR studies of the serine proteases. *Annu. Rev. Biophys. Bioeng.* 11:419–444.

Teeter, M. M., and D. A. Case. 1990. Harmonic and quasiharmonic descriptions of crambin. *J. Phys. Chem.* 94:8091–8097.

Verlet, L. 1967. Computer experiments on classical fluids. *Phys. Rev.* 159:98–113.

Verma, C. S., L. S. D. Caves, R. E. Hubbard, and G. C. K. Roberts. 1997. Domain motions in dihydrofolate reductase: a molecular dynamics study. *J. Mol. Biol.* 266:776–796.

Warshel, A. 1991. Computer Modeling of Chemical Reactions in Enzymes and Solution. John Wiley and Sons, New York.

Warshel, A. 1998. Electrostatic origin of the catalytic power of enzymes and the role of preorganized active sites. *J. Biol. Chem.* 273: 27035–27038.

Warshel, A., and J. Florian. 1998. Computer simulations of enzyme catalysis: finding out what has been optimized by nature. *Proc. Natl. Acad. Sci. USA.* 95:5950–5955.

Warshel, A., G. Naray-Szabo, F. Sussman, and J.-K. Hwang. 1989. How do serine proteases really work? *Biochemistry.* 28:3629–3637.

Warshel, A., and A. Papazyan. 1996. Energy considerations show that low-barrier hydrogen bonds do not offer a catalytic advantage over ordinary hydrogen bonds. *Proc. Natl. Acad. Sci. USA.* 93:13665–13670.

Warshel, A., A. Papazyan, and P. A. Kollman. 1995. On low-barrier hydrogen bonds and enzyme catalysis. *Science.* 269:102–104.

Warshel, A., F. Sussman, and J.-K. Hwang. 1988. Evaluation of catalytic free energies in genetically modified proteins. *J. Mol. Biol.* 201: 139–159.

Wells, J. A., B. C. Cunningham, T. P. Graycar, and D. A. Estell. 1986. Importance of hydrogen-bond formation in stabilizing the transition state of subtilisin. *Philos. Trans. R. Soc. Lond. A.* 317:415–423.